

EFFECTS OF CONSTRAINTS ON GAS FLOW ON THE SEVERITY OF VAPOUR CLOUD EXPLOSIONS[†]

Graham Atkinson

Fire and Process Safety Unit, Health and Safety Laboratory, Buxton, SK17 9JN, U.K

The flame speed and overpressure in a vapour cloud explosion depend on the extent to which movement of burned and/or unburned gas is constrained by solid surfaces or geometric factors. In general if the burned gas is constrained (prevented from moving) flame acceleration will be maximised. Such rapid acceleration occurs in linear flame spread in a pipe away from a closed end or spherical flame propagation from a point ignition. For flames propagating in the open or in an area where the density of obstacles is fairly uniform the level of constraint on unburned and burned gas is zero or equal. The tendency to flame acceleration is reduced and different relationships between flame speed and pressure apply.

The purpose of this paper is to demonstrate how the consideration of constraint can assist the interpretation of vapour explosion tests and improve the quality of hazard assessment.

STEADY FLAMES

The fundamental significance of flow constraint on explosion propagation is clearly illustrated by steady one-dimensional flame spread in a pipe. If movement of unburned gas is constrained (i.e. the flame is travelling towards a closed end) the flame speed is equal to the turbulent burning velocity S_u which is typically only a few metres per second. The expansion of gas during combustion drives a flow of burned gas backwards relative to the direction of explosion travel. On the other hand if the burned gas is constrained (propagation away from the closed end of a tube) expansion occurs as forward movement of the unburned gas. The flame speed is greater than the turbulent burning velocity by a factor equal to the expansion ratio $\sigma = \rho_u/\rho_b$.

These results are well known but there is a third significant special case in which there is no constraint on either burned or unburned gas or the level of constraint is similar. This corresponds to one-dimensional flame propagating in the open or through a uniform array of obstacles. In this case expansion drives unburned gas forwards and burned gas backwards. The flame speed exceeds the turbulent burning velocity by a factor of $\sqrt{\sigma}$. These three types of constraint are illustrated in Figure 1. Tables 1 and 2 show for each scenario the induced velocity in burned and unburned gas and the pressure across the flame.

It is worth noting that for the unconstrained flame the magnitude of dynamic pressure (which related to the drag on objects) is similar in the relatively slow but dense forward flow of unburned gas that precedes the flame arrival and the fast, low density backward flow of burned gas that follows it.

The pressure drop from unburned to burned gas is the same in all three cases – and proportional to the square of the turbulent burning velocity. This means that the pressure drop across the flame is a very different function of flame speed for different types of constraint.

In the case of constraint on burned gas (flame spread from a closed end) there is also a large general overpressure

that extends from the closed end through the burned and unburned gas to a shock that travels out ahead of the flame. The magnitude of this overpressure is (Landau 1959)

$$P_{\text{over}} = \frac{P - P_o}{P_o} = \frac{\gamma(\gamma + 1)M^2}{4} + M\gamma\sqrt{1 + \frac{(\gamma + 1)^2M^2}{16}} \quad (1)$$

Where M is the flame Mach number $M = V_f/V_{\text{sound}}$ and P_o is the absolute ambient pressure. For flame speeds much less than the speed of sound this expression becomes.

$$P_{\text{over}} = \rho_u \cdot V_{\text{sound}} \cdot V_f \quad (2)$$

This is much larger than the pressure across the flame, so in practice the burned and unburned gas are at almost the same high overpressure (Figure 2a).

Overpressures extending across both burned and unburned gas are also developed in the case of spherical flame spreading from a point ignition – although in this case the maximum pressures are much lower than for linear flame spread (by a factor V_f/V_{sound}). Moving out from the centre, through the burned gas, the pressure is constant in the burned gas, increases slightly across the flame front then declines with radius out through the unburned gas to the spherical shock expanding ahead of the flame (Figure 2b). There is no closed form solution for pressure in the spherical case but some typical results are given by Kuhl (1973). For relatively low flame speeds the maximum overpressure, at the outer edge of the flame, is approximately $(\rho_u - \rho_b) V_f^2$.

The typical distribution of pressure in an unconstrained or equally constrained steady flame in a congested array of width W_{array} is shown in Figure 2c. Well in advance

[†] © Crown Copyright 2012. This article is published with the permission of the Controller of HMSO and the Queen's Printer for Scotland.

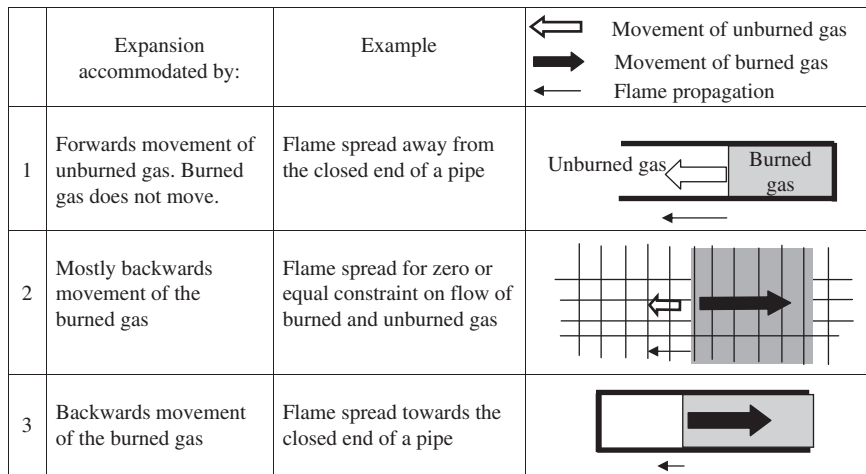


Figure 1. Flame spread and induced velocities for three types of constraint

of and behind the array the pressure relaxes by expansion outside the array: but conditions around the flame closely correspond to the one-dimensional case.

The negative pressure after the flame front in an unconstrained flame is typically small (Figure 2c) which means that measurements of maximum overpressure in an unconstrained flame typically return values close to the pressure drop across the flame. Figure 3 shows a variety of reported measurements of maximum overpressure in extended quasi-steady flames in congested arrays (Harrison and Eyre 1987; Harris and Wickens 1989; Van Wingerden 1989). As expected the relationship between maximum reported overpressure and flame speed corresponds reasonably closely to the pressure across the flame front in the ideal case with no constraint (i.e. no transfer of momentum from bounding surfaces).

Coincidentally the relationship between flame speed and maximum pressure in the unburned gas is very similar for the case of spherical and linear flames – which are two of the most common constraint geometries in practice. The same approximate formula $P \sim (\rho_u - \rho_b) V_f^2$ provides a useful rule of thumb linking flame speed to maximum overpressure in both cases. That this is simply a coincidence is illustrated by the fact that in an unconstrained linear flame the pressure drops rapidly to zero in the burned gas whereas in a spherical flame the pressure hardly changes as the flame passes.

FLAME ACCELERATION

The results for steady incompressible flames provide insights into the rate at which flames accelerate. The Schelkin mechanism involves the generation of turbulence as unburned gas is driven forwards past obstacles ahead of the flame. Turbulence increases the turbulent burning velocity, which increases the velocity of unburned gas ahead of the flame and so on. If there is constraint on burned gas in either linear or spherical geometry the forward velocity of the unburned gas and therefore the rate of flame acceleration will be maximised.

The relationships between turbulent intensity, forwards velocity and increased turbulent burning velocity is not straightforward. The increase in burning rate occurs partly through increased small scale mixing at the flame front and partly through the splitting and deformation of the flame front as it travels past obstacles. This produces a complex flame envelope with a large surface area over which the flame can consume unburned gas.

A number of simple relationships between turbulent intensity and burning velocity have been proposed. Although inevitably approximate (and generally restricted in relevance to one type of obstacle array) these relationships are worth pursuing because they allow solution of the flame spread problem. These solutions clearly illustrate the close relationship between constraint and flame speed (explosion severity).

Table 1. Flame speed and induced velocities for different types of constraint

	Flame speed V_f	Forward velocity of unburned gas V_{ug}	Backward velocity of burned gas
Burned gas stationary	$S_u \cdot \sigma$	$S_u \cdot (\sigma - 1)$	Nil
No constraint	$S_u \cdot \sigma^{1/2}$	$S_u \cdot (\sigma^{1/2} - 1)$	$S_u \cdot (\sigma - \sigma^{1/2})$
Unburned gas stationary	S_u	Nil	$S_u \cdot \sigma$

Table 2. Pressure drops across the flame for different types of constraint

	Pressure across flame front (as a function of S_u)	Pressure across flame front (as a function of V_f)
Burned gas stationary	$(\rho_u - \rho_b) \cdot \sigma \cdot S_u^2$	$1/\sigma \cdot (\rho_u - \rho_b) \cdot V_f^2$
No constraint	$(\rho_u - \rho_b) \cdot \sigma \cdot S_u^2$	$(\rho_u - \rho_b) \cdot V_f^2$
Unburned gas stationary	$(\rho_u - \rho_b) \cdot \sigma \cdot S_u^2$	$\sigma \cdot (\rho_u - \rho_b) \cdot V_f^2$

Gardner *et al.* (1998) propose the following relationship between the burning velocity and turbulent velocity induced by grids across the flame path where the Karlowitz number is greater than 1.

$$S_u = 5.15 R_L^{0.2} (\text{m/s}) \quad \text{Ka} > 1 \quad (3)$$

The turbulent Reynolds number $R_L \frac{V'_u \cdot D}{\nu}$ is a function of the rms turbulent velocity in the unburned gas V'_u , the turbulent length scale – assumed equal to the grid spacing D and the kinematic viscosity ν .

For high turbulent velocities these values of burning velocity are more than two orders of magnitude greater than the laminar flame speed and reflect both substantial increases in flame area as it passes through a grid and the rate at which burning progresses across this extended surface.

Figure 4 shows a graphical solution of the two Equations (3) and (4) linking the burning velocity and the forwards velocity of unburned gas for an unconstrained flame.

$$\text{Unconstrained flame} \quad V_u = S_u(\sigma^{1/2} - 1) \quad (4)$$

$$\text{Burned gas constrained} \quad V_u = S_u \cdot \sigma \quad (5)$$

Also shown on the same plot is the solution of equation (3) and (5) for a flame where the burned gas is constrained. In Figure 4 it is assumed the $D = 0.05 \text{ m}$, $\sigma = 7.5$ and the turbulence intensity downstream of the grid is so large that $V'_u/V_u \sim 0.5$.

Figure 4 suggests that where there is no constraint, a steady flame can propagate with a burning velocity of around 55 m/s, which corresponds to a flame speed of 150 m/s. On the other hand for flames with constraint on

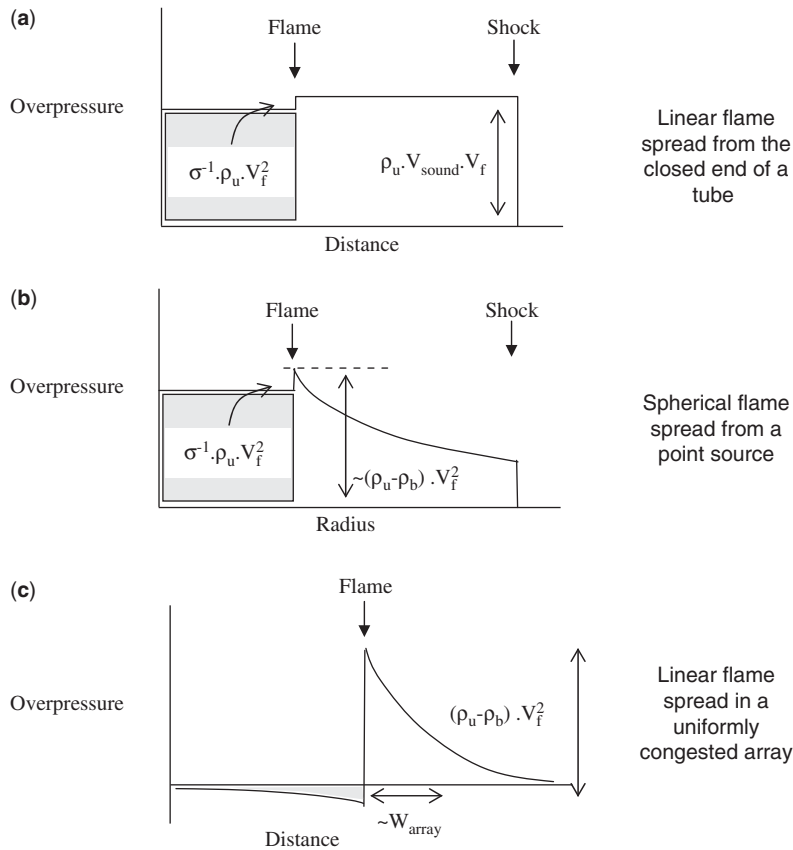


Figure 2. Pressure distributions in three different geometries. Explosion propagation is from left to right

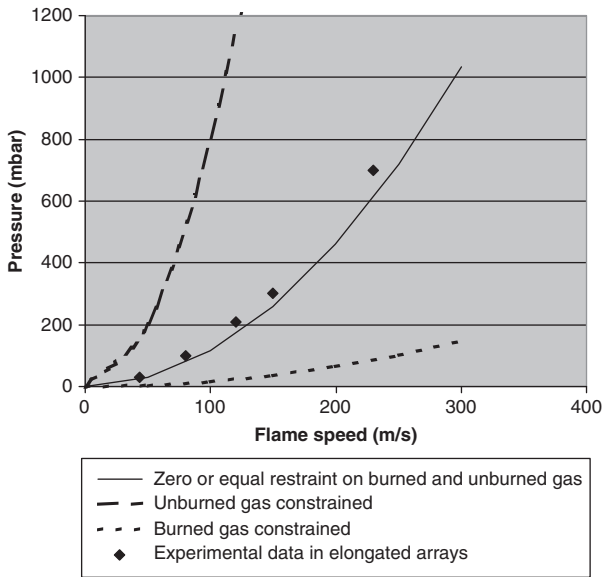


Figure 3. Theoretical estimates of pressure drop across the flame front and experimental measurements of flame speed and maximum overpressure.

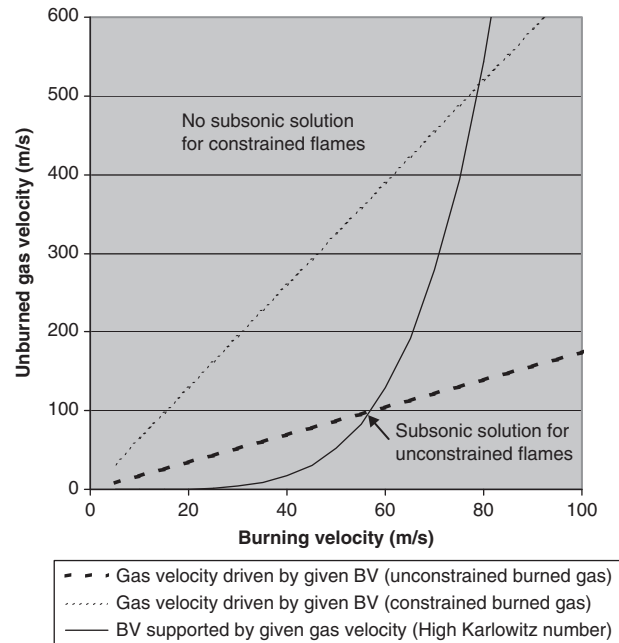


Figure 4. Prediction of burning velocity for flames without constraint and for those where burned gas is constrained

burned gas (i.e. confined in a tube or spreading spherically) there is no sub-sonic solution.

In practice such constrained flames typically accelerate rapidly beyond the range of applicability of Equations (3) and (5). At high (supersonic) speeds the ignition process is increasingly strongly affected by the adiabatic heating that accompanies the passage of shocks especially as these interact with shocks reflected from obstacles. Eventually the flame may undergo deflagration to detonation transition.

Some additional low speed solutions for the equations for unconstrained flame spread for different obstacle sizes and turbulent intensities are shown in Table 3. In all cases $\sigma = 7.5$.

FLAME ACCELERATION IN NARROW LINEAR ARRAYS (E.G. PIPE BRIDGES, HEDGES)

Following ignition within a congested array the flame initially spreads in a spherical manner. There is full constraint

on the burned gas and the rate of flame acceleration is large (Figure 5). As the flame reaches the edge of the array the area of the flame over which reaction is occurring becomes ever smaller as a proportion of the total surface area of the envelope of burned gas over which expansion can occur. Ever smaller pressures are required to drive the expansion of the burned gas and the effective level of constraint falls. Eventually the flame is effectively unconstrained: pressures and velocities are related to the burning velocity by the Equations in Tables 1 and 2. The distance over which the decline in the level of constraint occurs is of order five times the width of the array.

If flame acceleration is sufficiently rapid in the early, constrained phase of spread the flame may enter a self-sustaining, high speed burning regime where ignition and flame spread are strongly enhanced by shock compression. Once established such flames are not affected by the condition of the burned gas in the far-field and the flame continues at high speed whatever the length of the array.

Table 3. Steady low speed flames for different length scales and turbulent intensities

Turbulent length scale (mm)	Burning velocity at different turbulent intensities		
	100% $V'_u = V_u$	50% $V'_u = 0.5 V_u$	25% $V'_u = 0.25 V_u$
1000	145 m/s	120 m/s	100 m/s
100	80 m/s	65 m/s	55 m/s
10	45 m/s	40 m/s	35 m/s



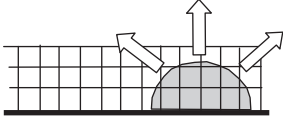
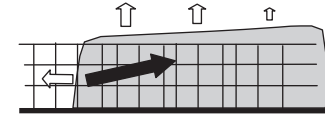
Expansion accommodated by:	Scenario	 Movement of unburned gas  Movement of burned gas
Outwards movement of the unburned gas	Initial accelerating stages of flame spread in an elongated congested array e.g. pipe bridge or hedge.	
Mostly backwards movement of the burned gas	Later steady stages of flame spread in an elongated array.	

Figure 5. Change in constraint as flame progresses through a narrow linear array

If acceleration is not so large, the effects of shock heating on ignition may not be felt before the level of constraint falls and reduces the tendency to flame acceleration. The flame settles into a steady low speed regime. This link between the rate of acceleration and the final burning regime was noted by TNO (Mercx *et al.* 1998). A corollary of TNO’s hypothesis is that acceleration to high speeds in a uniform array will occur rapidly – over a distance equal to a few times the width of the array – or not at all.

The development of two flames to the high and low burning regimes is illustrated in Figure 6.

This type of behaviour means that the relationship between final explosion strength and the properties of obstacles or gas is highly non-linear with large jumps in pressure for small changes in conditions (Figure 7). Development of an understanding of the form of the function P_{max} ($VBR, D_{obs}, S_L, W_{array}$) for central point ignition is a key challenge in industrial explosion assessment.

Significant progress has been made in obtaining an empirical understanding of the maximum pressure developed by a spherical flame as a function of the flame length $P_{max-spherical}$ ($VBR, D_{obs}, S_L, L_{flame}$). The GAMES

methodology for explosion assessment is based on this work via Equation (6) (Eggen 1995).

$$\Delta P(bar) = 0.84 \left(\frac{VBR \cdot L_{flame}}{D_{obs}} \right)^{2.75} \cdot S_L^{2.7} \cdot D_{obs}^{0.7} \quad (6)$$

TNO (Mercx 1998) have suggested that if the pressure exceeds 30 kPa in a narrow array at the point when the flame first reaches the edge of the array (calculated via Equation (6)) then ongoing flame acceleration will be quick enough that the effects of falling constraint will be overcome and a high speed flame will result. Unfortunately there is no clear evidence for this value; which was proposed simply as a pragmatic guide to the application of the GAMES method to narrow arrays.

Since then a number of additional experimental programmes have been carried out notably by Baker Risk (Pierorazio 2005). This work has established some combinations of VBR, D_{obs}, S_L and W_{array} that lead to steady low speed flames and some that lead to high speed flames however

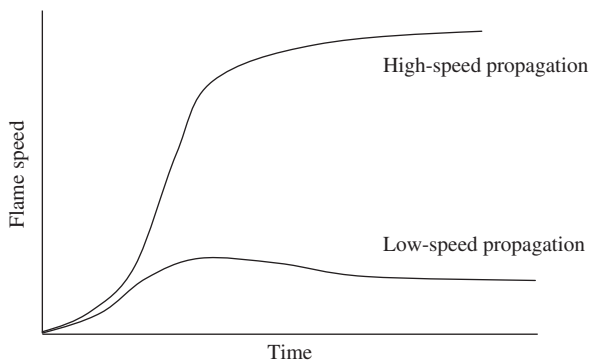


Figure 6. Development of flames into high-speed and low-speed burning regimes

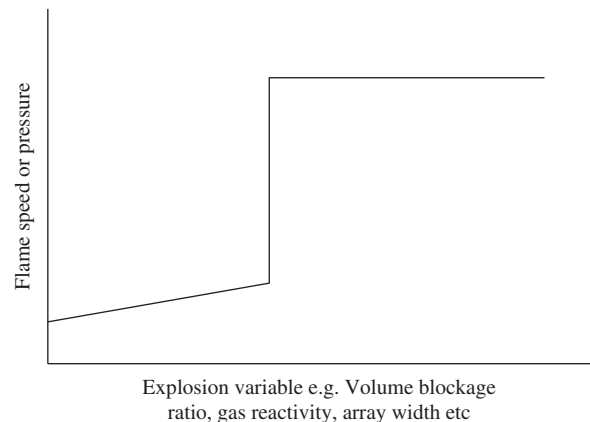


Figure 7. Schematic showing variation of explosion severity with important variables

the sum of the work falls well short of a full empirical theory.

The state of the art of CFD explosion modelling is improving but does not yet provide a reliable means for determining whether high speed flames or detonation are likely in a given case.

EFFECTS OF IGNITION SCENARIO

The worst-case (point source) ignition scenario for a given narrow array corresponds to ignition in the centre of the array. In this case the level of constraint is maximised for the longest possible time and the flame is most likely to reach the high-speed regime. If, however, ignition occurs not within the array, but in a distant uncongested part of a large vapour cloud, then the flame will enter the congested array across a broad front. Such a distant ignition is generally very much more likely in a real plant than point ignition deep within a heavily congested area.

In the case of flame entering the array across a broad front the level of constraint will be much lower: efficient backward venting of the explosion into the light burned gas can occur immediately. This causes minimal expansion of the total burned gas envelope requiring low pressures and exerting minimal constraint.

There is consequently a new function P_{max} (VBR, D_{obs} , S_L , W_{array}) corresponding to distant ignition. A significant proportion of congested arrays that will cause high intensity explosions for internal ignitions will not do so for distant ignitions. This is illustrated in Figure 8. In fact, analyses of the kind illustrated in Figure 4 suggest that (for congested arrays where the obstacle of size is less than a metre) once sub-sonic flame propagation is established it is very unlikely that further acceleration to the high speed regime can ever occur – even if the volume blockage ratio increases to very high levels.

Conversely, if ignition occurs in part of the cloud confined by solid boundaries (a bang box) reaching the high-speed regime is much more likely. If jet flames from the

bang box are directed down the line of a congested narrow array, the level of constraint on burned gas is high and will decline much more slowly than is the case when a spherical flame reaches the edge of an array. Consequently a broader range of array variables will correspond to flames that reach the high-speed regime.

POTENTIAL FOR FLAME ACCELERATION TO THE HIGH SPEED REGIME IN 2D ARRAYS E.G. EXTENDED CONGESTED PIPE ARRAYS, FORESTS

The above analysis of flame acceleration in linear arrays can be generalised to include 2D arrays by defining a *venting ratio*: this is the ratio between the area available for active explosion propagation (in congested linear or 2D array) and total surface area available for venting of burned gas. When the venting ratio is high the burned gas is relatively confined, forcing unburned gas ahead of the flame and promoting flame acceleration. For a spherical flame the venting ratio remains at unity whatever the flame diameter.

Figure 9 illustrates the progress of a flame through a shallow gas cloud in various linear and 2D congested arrays. In all cases the depth of the flammable cloud is H and the length of propagation of the flame L . For linear clouds the width is also H .

Generally the venting ratio falls as L increases – i.e. the explosion progresses. If the flame reaches a critical velocity (of order the speed of sound) before the venting ratio falls to a level of order $1/10$, then high-speed flame propagation and detonation may occur. If not a steady, low speed (sub-sonic) flame is likely.

For a given congestion density, flames propagating into 2D arrays accelerate for longer and are more likely to reach a high-speed burning regime. This is especially true if ignition occurs outside the array.

VELOCITY AND PRESSURE RELATIONSHIPS FOR AN EXTENDED REACTION ZONE

The relationships described in Tables 1 and 2 between burning velocity and flame speed, pressure etc. are only directly applicable to flames where the reaction zone is thin compared with the array width. When this is no longer the case there may be substantial sideways venting of reacting gas. The forward velocity of the unburned gas and flame speed both fall as a proportion of the burning velocity. A similar analysis to that carried out on thin flames predictably leads to lower flame speeds. The figures in Table 3 are therefore maximum values corresponding to the limit of thin flame sheets.

CONCLUSIONS

For 3D congested arrays (in deep vapour clouds) flames accelerate continuously and if the array large enough a high speed burning regime will be reached and there may be DDT.

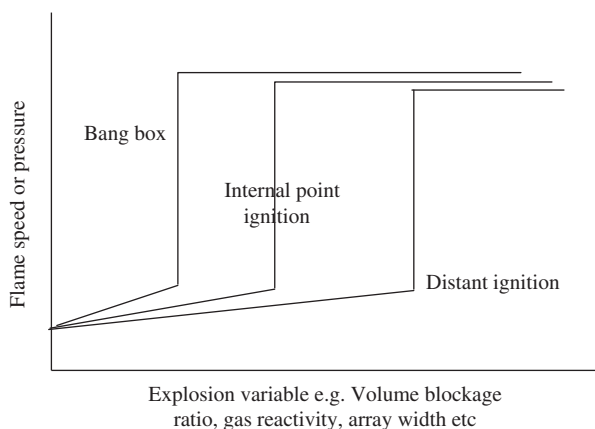


Figure 8. Schematic showing explosion severity for different ignition scenarios

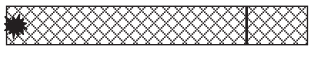
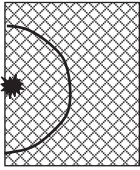
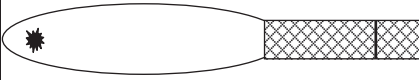
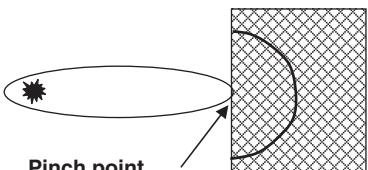
Scenario	Schematic	Venting Ratio	Flame acceleration potential
Ignition in a heavily congested linear array	 Ignition Flame front	$\frac{H}{3L}$	High
Ignition in a heavily congested 2D array		$\frac{2H}{L}$	Very high
Ignition in a lightly congested (or uncongested) area. Explosion entering heavily congested linear array		$\ll \frac{H}{3L}$	Low
Ignition in a lightly congested (or uncongested) area. Explosion entering heavily congested 2D linear array	 Pinch point prevents venting of burned gas into external hot gas envelope	$\frac{2H}{L}$	Very high

Figure 9. Comparison of venting ratios for linear and 2D arrays

For a shallow cloud in a 2D congested array (e.g. congested plant or a forest) the flame may reach a high speed regime but only if the obstacle density is high enough to raise the flame speed to roughly sonic speed within a distance of a few times the depth of the cloud. Otherwise the flame speed will be low, however large the array. In this (2D) case ignition outside the heavily congested region can lead to high flame speeds when the flame reaches the array.

For a shallow cloud in a linear array the flame must also accelerate quickly if it is to reach the high-speed regime. In this case ignition outside a heavily congested linear array will generally not lead to high speed burning when the flame arrives. This is relevant to the assessment of risk in sites where there are congested pipe runs or hedges in which ignition is very unlikely.

DISCLAIMER

This publication and the work it describes were funded by the Health and Safety Executive (HSE). Its contents, includ-

ing any opinions and/or conclusions expressed, are those of the authors alone and do not necessarily reflect HSE policy.

NOMENCLATURE

- γ Ratio of specific heats (unburned gas)
- ρ_u Density of the unburned gas (kg/m^3)
- ρ_b Density of the burned gas (kg/m^3)
- σ Expansion ratio ρ_u/ρ_b
- D_{obs} Diameter of obstacles (m)
- D Length scale of turbulence (m)
- H Height and width of a linear array
- Ka Karlovitz number $0.157 \left(\frac{V_f'}{S_L}\right)^2 R_L^{-0.5}$
- L, L_{flame} Distance of propagation of a flame (m)
- M Flame Mach number $M = V_f/V_{\text{sound}}$
- P_o Absolute ambient pressure (N/m^2)
- P_{over} Explosion pressure over ambient (N/m^2)

R_L	Turbulence Reynolds number $\frac{V'_u \cdot D}{\nu}$
S_L	Laminar flame speed (m/s)
S_u	Turbulent burning velocity (m/s)
V_u	Velocity of unburned gas
V'_u	RMS turbulent velocity in unburned gas
VBR	Volume blockage ratio for obstacle array
V_f	Flame speed (m/s)
V_{sound}	Speed of sound in the unburned gas (m/s)
W_{array}	Width (and height) of a long array (m)

REFERENCES

- Eggen, J.B.M.M. (1995) *GAME: development of guidance for the application of the multi-energy method*. TNO Report 1995-C44.
- Gardner, C.L., Phylaktou, H. and Andrews, G.E. (1998) *Turbulent Reynolds number and turbulent flame quenching influences on explosion severity with implications for explosion scaling*, IChemE Symposium Series No. 144. pp. 279–292, Paper 23.
- Harris, R.J. and Wickens, M.J. (1989) *Understanding vapour cloud explosions – an experimental study*. 55th Autumn Meeting of the Institution of Gas Engineers, Kensington, U.K.
- Harrison, A.J. and Eyre, J.A. (1987) *The effects of obstacle arrays on the combustion of large pre-mixed gas/air clouds*. Comb. Science and Tech, Vol. 52, pp. 121–137.
- Kuhl, A.L., Kamel, M.M. and Oppenheim A.K. (1973), *Pressure waves generated by steady flames*. Fourteenth International Symposium on Combustion, pp. 1201–1215.
- Landau, L.D. and Lifshitz, E.M. (1959), *Fluid Mechanics*, Pergamon Press, Oxford.
- Mercx, W.P.M., van den Berg, A.C., and van Leeuwen, D. (1998) *Application of correlations to quantify the source strength of vapour cloud explosions in realistic situations: Final report for the project: 'GAMES'* TNO Report 1998-C53.
- Pierorazio, A.J., Thomas J.K., Baker, Q.A. and Ketchum D.E. (2005) *An update to the Baker-Strehlow-Tang Vapor Cloud Explosion Prediction Methodology Flame Speed Table*. Process Safety Progress, Vol. 24, No. 1. pp. 59–65.
- Wingerden, C.J.M van, (1989) *Experimental investigation into the strength of blast waves generated by vapour cloud explosions in congested areas*. 6th Int. Symp. on Loss Prevention and Safety promotion in the Process Industries. Paper 26, pp. 1–16.